RSC Advances

PAPER

View Article Online
View Journal | View Issue

Cite this: *RSC Adv.*, 2016, **6**, 6516

A graphene quantum dot (GQD) nanosystem with redox-triggered cleavable PEG shell facilitating selective activation of the photosensitiser for photodynamic therapy†

Yan Li,‡[a] Zhiyong Wu,‡[b] Dou Du,[a] Haiqing Dong,[a] Donglu Shi*[ac] and Yongyong Li*[a]

Received 9th November 2015
Accepted 23rd December 2015

DOI: 10.1039/c5ra23622c

www.rsc.org/advances

In photodynamic therapy (PDT), selective activation of the photosensitiser in tumor-relevant conditions is highly desirable to avoid side effects. In this study, a graphene quantum dot (GQD) nanosystem, composed of a redox-triggered cleavable PEG shell, was designed and developed for selective recovery of photoactive chlorine e6 (Ce6) in tumor-relevant conditions. In this unique system, the planar π conjugated structure of GQD enables efficient quenching of the photochemical properties of Ce6 in terms of fluorescence and singlet oxygen generation. Once exposed to tumor relevant glutathione (GSH), the disulfide-linked PEG shell undergoes reductive cleavage and subsequent detachment from the GQD scaffold, leading to accelerated release of Ce6 with recovered photoactivity. MTT study against HeLa cells demonstrated the high PDT efficacy of Ce6, regulated by elevated GSH concentration. The studies on *in vivo*/*ex vivo* imaging and photodynamic efficacy demonstrated superior biocompatibility of the GQD nanosystem compared with the widely reported graphene oxide (GO)-based nanovehicle. Intravenously injected GQD–SS–PEG/Ce6 showed effective suppression of tumor growth.

Introduction

Photodynamic therapy (PDT), a minimally invasive approach, which utilizes light as exterior stimulator to activate a photosensitizer (PS) for therapy, has been extensively investigated for its clinical importance, especially in the treatment of superficial tumors.[1] However, healthy organs or tissues exposed to environmental light may suffer from some degree of phototoxicity upon administration of the photosensitizer.[2] It is, therefore, important to regulate the photoactivity of the PS in order to minimize the off-target phototoxicity. Thus it would be ideal to temporally quench the fluorescence and phototoxicity of the PS before reaching the target tumor sites. Fluorescence resonance energy transfer (FRET) has been utilized to target-activation of the photoactivity of the PS. The principle is based on incorporation of a disease-specific linker between the $^1O_2$ quencher and PS. This linker can be cleaved by certain biochemistry variations at the lesion, consequently releasing the photoactive PS. For example, peptide linkers responsive to specific cancer-associated protease have been utilized to construct protease-controlled singlet oxygen quenching and activation photosensitizing beacon.[3–5] In this study, a redox-triggered photosensitizing beacon was designed *via* a disulfide linker between the $^1O_2$ quencher graphene quantum dot (GQD) and PS chlorine e6 (Ce6).

GQD has been emerging as a promising material for biomedical applications.[6,7] GQD resembles the graphene structure with single or a few layers of sp^2 hybridized carbon atoms packed into a unique planar structure, making it an ideal platform of FRET.[8,9] In addition to the remarkable physicochemical properties of graphene oxide (GO), GQD has more periphery carboxylic groups, smaller lateral size, and tunable photoluminescence. GQD has been extensively explored for cellular imaging and drug delivery due to its intrinsic fluorescence and characteristic planar surface for π–π interactions.[10–13] Moreover, owing to its small size, GQD was shown to be more compatible with the biological system.[14,15] Zhang *et al.*[15] have demonstrated superior biocompatibility of GQD–PEG *in vivo*, due to fast clearance of ultra-small GQD–PEG. On the contrary, GO–PEG exhibited significant toxicity, causing death due to GO aggregation in main organs of mice. Biosafety of GQDs may possibly be associated with their fast clearance through kidneys without generating toxic moieties.

[a]*Shanghai East Hospital, The Institute for Biomedical Engineering & Nano Science (iNANO), Tongji University School of Medicine, Shanghai, P. R. China. E-mail: yongyong_li@tongji.edu.cn*

[b]*Tongji University School of Materials Science and Engineering, Shanghai, P. R. China*

[c]*The Materials Science and Engineering Program, College of Engineering and Applied Science, Department of Mechanical and Materials Engineering, University of Cincinnati, Cincinnati, OH 45221, USA. E-mail: donglu.shi@uc.edu*

† Electronic supplementary information (ESI) available: Preparation and characterization of GQD–PEG–Ce6 and GO–PEG–Ce6. See DOI: 10.1039/c5ra23622c

‡ Authors Yan Li and Zhiyong Wu contributed equally to this work.

Considering the therapeutic requirements, particularly in a clinical setting, a new GQD system was developed in this study that featured a redox-triggered detachable PEG shell. The design of the nanostructure was tailored to the specific requirements for the selective recovery of photoactive Ce6 in tumor-relevant conditions. Fig. 1 is the schematic diagram showing the structural design, cell endocytosis, and intracellular Ce6 release of GQD–SS–PEG nanosystem. A PS-loaded GQD system is inert due to the quenching effect. Its photochemical property can be recovered by PEG detachment in tumor-relevant conditions. The PEG shell is connected to GQD *via* a disulfide linkage (GQD–SS–PEG) that can respond to changes in glutathione (GSH) for redox-activated PS delivery. The intercellular and intracellular GSH variation, as well as the difference between the tumor and normal cells has been extensively utilized for triggering drug release.[16]

Experimental

Chemicals

H_2SO_4 (AR, 98%), $NaNO_3$ (AR), H_2O_2 (AR, 30%), $KMnO_4$ (AR) were supplied by Sinopharm Chemical Reagent Co. Ltd. Graphite was obtained from Shanghai Yifan Graphite Co., Ltd. Methoxy PEG carboxyl (CH_3O–PEG–COOH, Mn: 5000), and *t*-Boc amine PEG amine (Boc–PEG–NH_2, Mn: 3500) were purchased from JenKem Technology Co., Ltd. Cystamine dihydrochloride (98%), *N*-hydroxysuccinimide (NHS, 98%), 1-ethyl-3-(3-dimethylaminopropyl) carbodiimide hydrochloride (EDC·HCl, 98.5%), glutathione (GSH, 98%), trifluoroacetic acid (TFA, 99%), dithiothreitol (DTT), dichloromethane (DCM), ethyl ether, and dimethyl sulfoxide (DMSO) were obtained from Aladdin Chemistry Co. Ltd. Singlet Oxygen Sensor Green (SOSG) was obtained from Life Technologies. The photosensitiser Ce6 was obtained from J&K Scientific Ltd. Triethylamine was purchased from Sigma-Aldrich Co. LLC. Glutathione reduced ethyl ester (GSH-OEt) was obtained from Sigma-Aldrich. Fetal bovine serum (FBS), Dulbecco's modified Eagle's medium (DMEM), penicillin–streptomycin, 3-(4,5-dimethylthiazol-2-yl)-2,5-diphenyltetrazolium bromide (MTT), trypsin, and Dulbecco's phosphate-buffered saline (DPBS) were supplied by Gibco Invitrogen Corp. Co. Ltd. 4,6-Diamidino-2-phenylindole (DAPI) was obtained from Beyotime Institute of Biotechnology. Paraformaldehyde (4%) was obtained from DingGuo Chang Sheng Biotech.

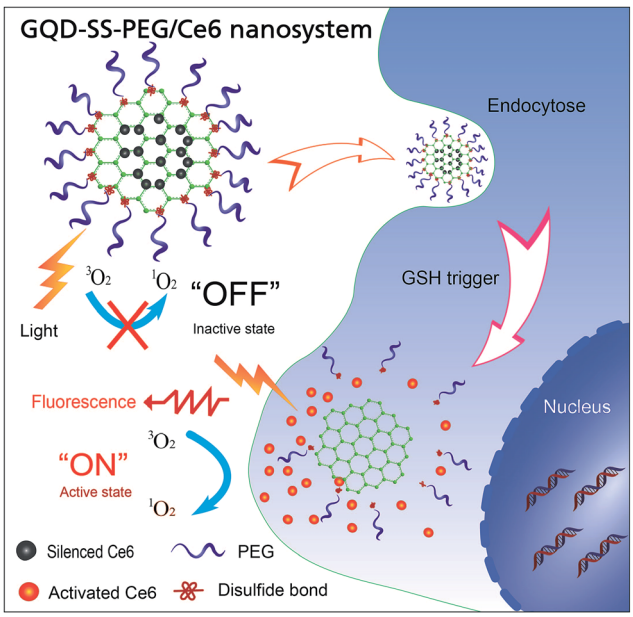

Fig. 1 Schematic diagram of the structural design, cell endocytosis, and intracellular Ce6 release of GQD–SS–PEG nanosystem.

Characterization

UV-vis, fluorescence spectra and Fourier transform infrared (FTIR) spectra were collected by an UV-vis spectrophotometer (Varian, Cary 50), a fluorescence spectrometer (PerkinElmer, LS-55) and a FTIR spectrometer (Bruker, Tensor 27), respectively. The particle size distribution and morphology were obtained with laser diffraction-based particle size analyzer (Malvern, NanoZS90) and transmission electron microscopy (TEM) (Netherlands, Tecnai 12), respectively. The cellular uptake was monitored by Confocal Laser Scanning Microscope (CLSM) (Germany, Leica TCS SP5 II).

Preparation of GQD

GQD was synthesized according to the direct oxidizing and etching method.[17]

Preparation of PEG–SS–NH_2

PEG–SS–NH_2 was obtained according to the reported procedure.[18]

Preparation of PEGylated GQD with a disulfide linkage (GQD–SS–PEG)

100 mg PEG–SS–NH_2 was added to a mixture of 10 mg EDC·HCl and 10 mL GQD (1 mg mL^{-1}) which was sonicated for 5 min. The above suspension was stirred overnight at ambient temperature and then dialyzed to get GQD–SS–PEG.

Loading of Ce6 onto GQD–SS–PEG

The loading of Ce6 was accomplished by simply mixing GQD–SS–PEG with the given amount of Ce6. In detail, Ce6 was first sonicated with 10 mL GQD–SS–PEG aqueous solution (1 mg mL^{-1}) for 30 min. The above mixture was stirred at ambient temperature overnight and centrifuged. Finally the supernatant was transferred to a millipore and ultrafiltered to remove free Ce6. The amount of Ce6 entrapped in GQD–SS–PEG was obtained by measuring the UV absorbance at 405 nm and the absorbance of GQD at the same wavelength was subtracted.

GSH-induced Ce6 *in vitro* release

The GSH-induced Ce6 release was studied in 2 μM or 10 mM GSH solution. At predetermined time intervals, 2 mL solutions were withdrawn and replaced with 2 mL fresh GSH solution.

The Ce6 concentration was determined by measuring the fluorescence spectra (excitation at 405 nm).

Fluorescence and singlet oxygen generation assay

Fluorescence measurements were performed by measuring the intensity of free Ce6 released from the GQD–SS–PEG after the addition of 1 mM DTT. To evaluate the inhibitory and recovery characteristics with respect to singlet oxygen generation, singlet-oxygen-detecting reagent SOSG was dissolved in PBS containing GQD–SS–PEG/Ce6, GQD–SS–PEG/Ce6 treated with 10 mM GSH for 3 h or free Ce6. The final concentration of Ce6 and SOSG were maintained at 1 μM. Irradiation was performed with a CW laser beam of 650 nm at 20 mW cm^{-2}.

In vitro phototoxicity test of free Ce6, GQD–SS–PEG and Ce6 loaded GQD–SS–PEG

HeLa cells were cultivated in 96-well plates for 24 h. Then free Ce6, GQD–SS–PEG and Ce6 loaded GQD–SS–PEG at 0.25, 0.5, 1, 2 μM Ce6 equivalent concentrations were added for 6 h incubation, before irradiation with laser beam of 650 nm at 20 mW cm^{-2}. The irradiation lasted for 3 min. After irradiation, cells were cultivated for another 24 h. Cell viabilities were determined by MTT assay. Dark toxicity of the free Ce6, GQD–SS–PEG and Ce6 loaded GQD–SS–PEG was carried out by incubating these compounds for 24 h without light treatment.

Redox-dependent *in vitro* phototoxicity test of Ce6 loaded GQD–SS–PEG

After HeLa cells were cultivated for 24 h, 10 mM GSH-OEt was first added for 2 h incubation. Then the cells were washed with PBS and cultivated with Ce6 loaded GQD–SS–PEG of different Ce6 concentrations (100 μL; 0.25, 0.5, 1, 2 μM) in complete DMEM for an additional 24 h. After replacing with fresh DMEM (100 μL), cells were irradiated with laser beam of 650 nm at 20 mW cm^{-2} for 3 min. After irradiation, cells were cultivated for another 24 h. Then cell viabilities were determined by MTT assay.

Cellular uptake of Ce6 loaded GQD–SS–PEG and free Ce6

HeLa cells were incubated on cover glasses in 24-well plates for 24 h. Then Ce6 loaded GQD–SS–PEG or free Ce6 (Ce6 concentration of 1.5 μM) was added to cells. The culture medium was removed after 6 h cultivation, and cells were washed with DPBS, fixed with 4% paraformaldehyde for 10 min, and stained with DAPI for 3 min before rinsing with DPBS. Cells were imaged by CLSM.

Redox-dependent intracellular drug release of Ce6 loaded GQD–SS–PEG

HeLa cells were incubated on cover glasses for 24 h. 10 mM GSH-OEt was then added for 2 h continued incubation. The cells were washed with PBS and cultivated with Ce6 loaded GQD–SS–PEG. After 6 h cultivation, the culture medium was removed. The following fixation, staining and imaging process was carried out in the same way as the previous step.

In vivo fluorescence imaging of GQD–PEG–Ce6 and GO–PEG–Ce6

All experiments involving live animals were carried out according to protocols approved by the institutional committee for animal care, and also in compliance with the guidelines of the Institutional Animal Care and Use Committee of Tongji University. Tumor-bearing mice were obtained by subcutaneously injecting a suspension of 5×10^6 Hela cells into the right flank of six-week old female nude mice. After GQD–PEG–Ce6 and GO–PEG–Ce6 was intravenously administrated into mice, fluorescence imaging was performed with a NightOWL LB 983 IN-VIVO imaging system (Ce6 concentration: 10 mg kg^{-1}, tumor size: 3–5 mm in diameter, time point: 1 h, 4 h and 24 h). The tumors, hearts, lungs, spleens, livers, and kidneys were taken out and imaged in the same conditions.

Assay of *in vivo* antitumor efficacy

Mice bearing Hela tumor (tumor size: 3–5 mm in diameter) were divided into two groups. Group 1 was intravenously administered with 200 μL Ce6-loaded GQD–SS–PEG (dose of 2.5 mg kg^{-1} of Ce6). As control group, mice in group 2 received an intravenously injection of 200 μL PBS. After 1 h, mice were anesthetized and irradiated for 1 h with laser beam of 650 nm at 200 mW cm^{-2}. The tumor sizes were measured every other day after treatment. Tumor volume was calculated using the formula: $V = WL^2/2$ (W: the longest diameter, L: the shortest diameter).

Results and discussion

Synthesis and characterization of disulfide-linked PEG coated GQD–SS–PEG nanosystem

The synthetic route of GQD–SS–PEG is shown in Fig. 2. GQD was prepared by directly oxidizing graphite powders through two steps.[17] As shown in Fig. 2, the first step is to chemically oxidize

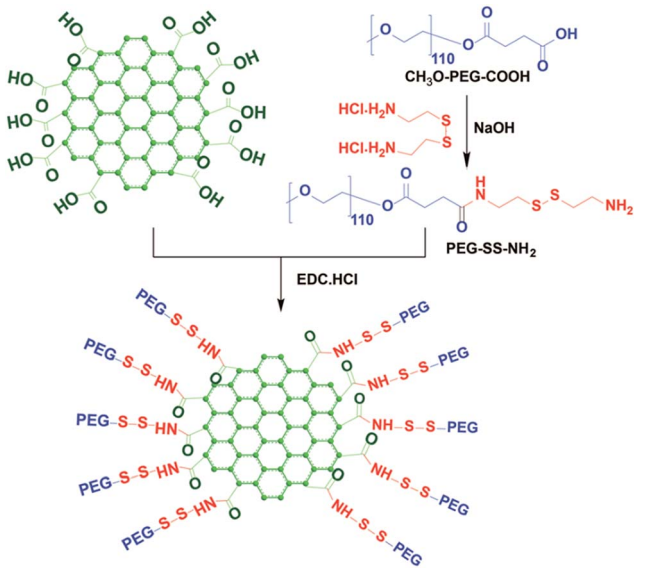

Fig. 2 Synthesis route of disulfide-linked GQD–SS–PEG.

graphite at 40 °C to GO. Step 2 further increases temperature of this reaction to 120 °C and refluxes for 12 h for reducing GO into nano-scaled dots. PEG–SS–NH_2 is then synthesized by reacting CH_3O–PEG–COOH with cystamine. Upon conjugating GQD with PEG–SS–NH_2, the final product GQD–SS–PEG is synthesized.

Fig. 3 shows the FTIR spectra of PEGylation of GQD. As shown in this figure, the absorption band at 1600 cm^{-1}, 1700 cm^{-1}, 3220 cm^{-1} and 3010 cm^{-1} corresponds to the aromatic C=C, C=O, O–H, Ar–H stretching peak of GQD respectively. Upon chemically bonding of PEG–SS–NH_2 on GQD, the characteristic band of GQD at 1600 cm^{-1} (aromatic C=C group) and PEG at 2887 cm^{-1} and 1104 cm^{-1} (C–H and C–O–C groups) emerges simultaneously, which indicates the integration of PEG moieties to GQD.

The TEM images of GQD and GQD–SS–PEG is shown in Fig. 4. The average diameter of GQD is 2–5 nm. While for GQD–SS–PEG, due to the attachment of PEG–SS–NH_2, the diameter increases to 3–10 nm.

Quench effect and redox accelerated release of Ce6

The second generation PS Ce6, which has been widely incorporated into drug carriers for PDT,[19] was selected as a model drug in this study. GQD–SS–PEG/Ce6 complex was prepared by mixing the GQD–SS–PEG aqueous solution with the Ce6/DMSO solution at room temperature followed by ultra-filtering against DD water. Fluorescence spectroscopy and UV spectrum were used to analyze the interactions between GQD–SS–PEG and Ce6. The UV absorption spectra of GQD–SS–PEG and GQD–SS–PEG/Ce6 are shown in Fig. 5a. GQD–SS–PEG/Ce6 solution shows the characteristic absorption bands of Ce6 at 405 and 655 nm, indicating successful loading of Ce6 onto GQD–SS–PEG.

The fluorescence intensities of Ce6 and GQD–SS–PEG/Ce6 are shown in Fig. 5b. As can be seen, the fluorescence of Ce6 is strongly quenched after loading onto GQD–SS–PEG, most likely due to FRET as a result of π–π stacking and hydrophobic interactions between GQD and Ce6.[20,21] However, with exposure to DTT, fluorescence intensity of Ce6 is restored due to cleavage of the disulfide bond of the GQD–SS–PEG nanocarrier by the reducing agent and subsequently accelerated Ce6 release (Fig. 5b).

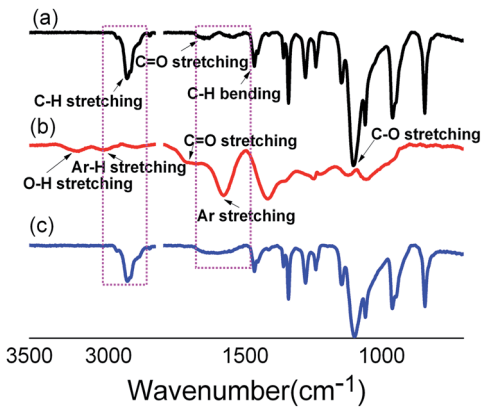

Fig. 3 FT-IR spectra of (a) PEG–SS–NH_2, (b) GQD and (c) GQD–SS–PEG.

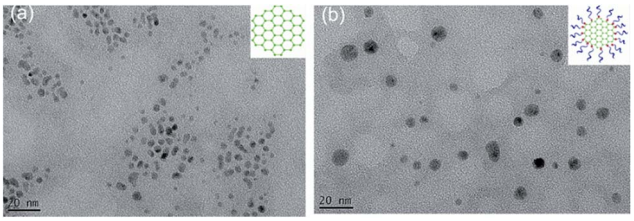

Fig. 4 TEM image of (a) GQD and (b) GQD–SS–PEG.

As shown in Fig. 5c, the accelerated release behavior of Ce6 upon redox triggering is also confirmed by the release curves at 2 μM and 10 mM GSH. For 10 mM GSH, GQD–SS–PEG/Ce6 shows a much faster drug release rate. 36% of Ce6 is released within 10 h. However, at 2 μM GSH, only 3% of loaded Ce6 is released throughout the period of 82 h. These results are consistent with our previous studies[18] that the release kinetics of graphene–drug nanosystem is modulated by cleavage of the PEG shell from the graphene architecture. This approach is shown to be an effective way of accelerating Ce6 release in tumor-relevant conditions.

Redox regulated recovery of photoactive Ce6

The influence of the redox-dependent nature of GQD–SS–PEG was investigated on the singlet oxygen generation of PS molecule Ce6. Its effect on the singlet oxygen generation abilities of GQD–SS–PEG/Ce6 was also investigated in the absence and presence of the reducing agent GSH under irradiation of a 650 nm laser (Fig. 5d). The singlet oxygen generation was detected by the singlet-oxygen-detecting reagent singlet oxygen sensor green (SOSG). Likewise, the generation of singlet oxygen was blocked by the aromatic GQD vehicle due to the energy transfer effect from excited Ce6 to GQD.[22] However, after treating GQD–

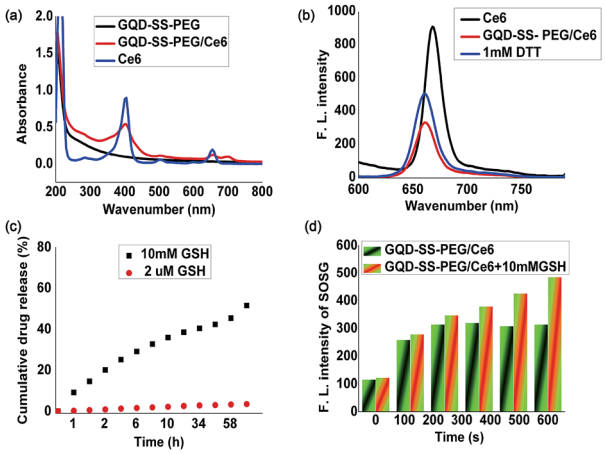

Fig. 5 (a) UV absorption spectra of GQD–SS–PEG and GQD–SS–PEG/Ce6; (b) fluorescence quenching and recovery of GQD–SS–PEG/Ce6; (c) GSH-mediated drug release from Ce6-loaded GQD–SS–PEG; (d) GSH-activated photoactivity of GQD–SS–PEG/Ce6.

SS–PEG/Ce6 with 10 mM GSH for 3 h, the singlet oxygen generation of Ce6 was effectively triggered due to the cleavage of the PEG shell from the graphene architecture and the subsequently Ce6 release.

Intracellular uptake and photodynamic effect *in vitro*

The PDT efficacy of Ce6-loaded GQD–SS–PEG was investigated by MTT assay. Hela cells were incubated for 24 h with GQD–SS–PEG/Ce6, GSH-pretreated GQD–SS–PEG/Ce6, GQD–SS–PEG, and Ce6 at various concentrations. The cells were then irradiated with a laser beam of 650 nm at 20 mW cm^{-2} for 3 min. The penetration at near infrared range can be significantly enhanced for PDT treatment. For the GSH-pretreated GQD–SS–PEG/Ce6 group, GSH-OEt was used to enhance the intracellular GSH level,[23] and cells were pretreated with 10 mM GSH-OEt for 2 h before the addition of GQD–SS–PEG/Ce6.

As shown in Fig. 6, without light exposure, GQD–SS–PEG, Ce6, GQD–SS–PEG/Ce6, and GSH-pretreated GQD–SS–PEG/Ce6 all exhibit no dark toxicity to Hela cells. GQD–SS–PEG without Ce6 was not toxic to Hela cell even under light irradiation. Surprisingly, the cancer cell killing effect of Ce6-loaded GQD–SS–PEG was much stronger than that of free Ce6 when irradiated by the 650 nm laser. The enhanced efficacy is associated with higher Ce6 cellular uptake assisted by GQD–SS–PEG compared with free Ce6, as shown in Fig. 7. For Ce6-loaded GQD–SS–PEG at higher Ce6 concentrations (2 μM), the passive uptake resulted in sufficient cells killing with or without the presence of GSH-OEt. However, at lower Ce6 concentrations (from 0.25 to 1 μM), the GSH-OEt addition enhanced the PDT effect of Ce6-loaded GQD–SS–PEG. This is especially beneficial for clinical applications as less drug is to be required for more pronounced therapeutic effect.

The cellular uptake behaviors of Ce6, GQD–SS–PEG/Ce6, and GSH-pretreated GQD–SS–PEG/Ce6 were studied by CLSM. Hela cells were cultured with GQD–SS–PEG/Ce6, GSH-pretreated GQD–SS–PEG/Ce6, and Ce6 for 6 h (Ce6 concentration: 1.5 μM). As shown in Fig. 7, cells cultured with GQD–SS–PEG/Ce6 display stronger Ce6 fluorescence due to high cellular uptake of GQD–SS–PEG/Ce6 which is associated with the effective endocytosis of GQD–SS–PEG.[21,24] In contrast, the uptake of free Ce6 without carrier into the cells is obviously slower. Compared with GQD–SS–PEG/Ce6, stronger Ce6 fluorescence is observed in the GSH-pretreated GQD–SS–PEG/Ce6 HeLa cells. The high intracellular GSH level has accelerated Ce6 release from the GQD–SS–PEG nanovehicle.

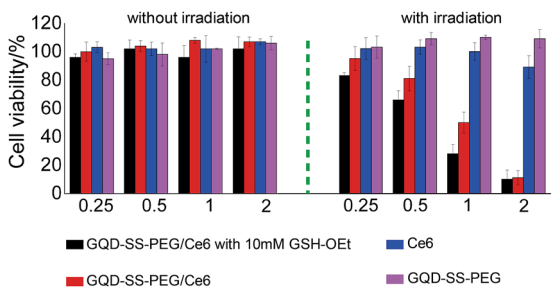

Fig. 6 Cell viability of HeLa cells incubated with GQD–SS–PEG/Ce6 with 10 mM GSH-OEt, GQD–SS–PEG/Ce6, Ce6 and GQD–SS–PEG without and with irradiation.

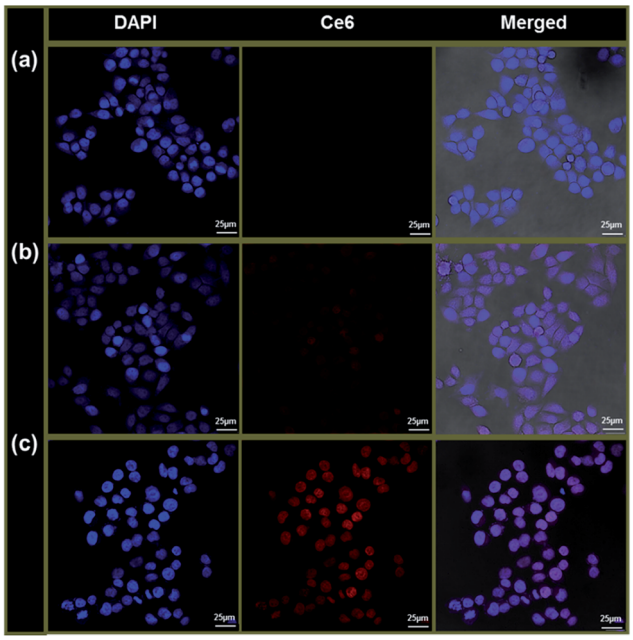

Fig. 7 Representative CLSM micrographs of (a) free Ce6, (b) GQD–SS–PEG/Ce6 and (c) GQD–SS–PEG/Ce6 with 10 mM GSH-OEt after 6 h incubation with HeLa cells.

In vivo and *ex vivo* optical imaging and biodistribution study

GQD–PEG has been reported for its superior biocompatibility compared with the widely used GO–PEG.[15] For *in vivo* behaviors, Ce6 was chemically conjugated on GQD–PEG and GO–PEG to avoid the interference of passively released Ce6. Detailed information about the preparation and characterization of GQD–PEG–Ce6 and GO–PEG–Ce6 can be found in the ESI.† The biodistribution of GQD–PEG–Ce6 and GO–PEG–Ce6 was monitored using Ce6 fluorescence. The mouse bearing Hela tumor was imaged at 1 h, 4 h and 24 h after being intravenously injected with GQD–PEG–Ce6 and GO–PEG–Ce6. Compared to GO–PEG–Ce6, GQD–PEG–Ce6 showed a higher tumor uptake. One hour after intravenous injection, the Hela tumor sites exhibited more intense fluorescence signal of Ce6 for the GQD–PEG–Ce6-treated group compared to the GO–PEG–Ce6-treated counterpart (Fig. 8a). With increasing time, the fluorescence signal of GQD–PEG–Ce6 decreased gradually due to fast clearance of ultra-small GQD–PEG–Ce6.[14,15] The biodistribution of intravenously injected GQD was also studied. It was found that GQD–PEG–Ce6 was mainly accumulated in kidneys with low distributions in other organs. This behavior suggests excretion of GQD–PEG–Ce6 mainly through kidney due to the small particle size of GQD around 5 nm. This is in accordance with the previously reported work.[25,26]

In vivo photodynamic anticancer effects of Ce6 by GQD–SS–PEG nanosystem

The anticancer efficacy of PDT was further evaluated by systemic delivery of GQD–SS–PEG/Ce6. Subcutaneous Hela

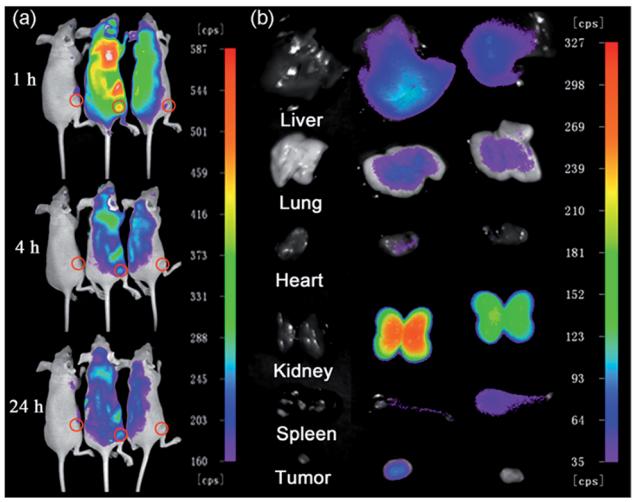

Fig. 8 (a) *In vivo* fluorescence images of nude mice bearing HeLa tumor after intravenous injection of PBS (left mouse), GQD–PEG–Ce6 (middle mouse) or GO–PEG–Ce6 (right mouse). The red circle indicates the position of tumor. (b) *Ex vivo* fluorescence images of liver, lung, heart, kidney, spleen and tumor after 24 h injection of PBS (left mouse), GQD–PEG–Ce6 (middle mouse) or GO–PEG–Ce6 (right mouse).

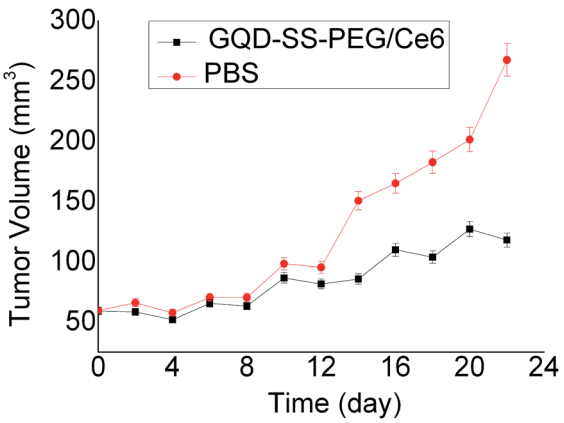

Fig. 9 *In vivo* antitumor application of GQD–SS–PEG/Ce6. PBS serves as control.

tumors exhibited significant differences in tumor growth rates when illuminated 1 h after intravenous administration of GQD–SS–PEG/Ce6 or PBS. The tumor size was measured every two days after treatment. The tumor volume of the GQD–SS–PEG/Ce6 group was 118 ± 6 mm^3 on day 22, while that of the PBS group on the same day had increased to 267 ± 13 mm^3. The tumor volume shows apparent suppressive effect of tumor growth in the GQD–SS–PEG/Ce6 treated group as compared to the PBS treated counterpart (Fig. 9).

Conclusions

A graphene quantum dot (GQD) nanosystem with cleavable PEG shell has been developed for selective recovery of photoactive chlorine e6 (Ce6) in tumor-relevant conditions. The system temporarily inactivates PS in normal condition while recovers the photoactive Ce6 in reduction glutathione (GSH) condition. GSH exposure initiates the detachment of the surface coated PEG shell by cleavage of the disulfide bond, subsequently accelerating the rapid release of Ce6 with recovered photoactivity. Regulation capability on photoactivity is clearly supported by physicochemical and cell proliferation assays with or without the presence of elevated GSH concentration. Intravenously injected GQD–SS–PEG/Ce6 shows apparent suppressive effect of tumor growth. These results suggest that the GQD-based and target-activated nanovehicle can serve as potential delivery system for PS with controlled photoactivity in a tumor-selective fashion and reduced side effects.

Acknowledgements

This work was financially supported by 973 program (2013CB967500), National Natural Science Foundation of China (81402884, 51473124, 51173136 and 21104059), Shanghai Rising-Star Program (12QA1403400), National Science Foundation for Post-doctoral Scientists of China (2014M561511, 2015T80453) and "Chen Guang" project founded by Shanghai Municipal Education Commission and Shanghai Education Development Foundation.

Notes and references

1 P. Agostinis, K. Berg, K. A. Cengel, T. H. Foster, A. W. Girotti, S. O. Gollnick, S. M. Hahn, M. R. Hamblin, A. Juzeniene and D. Kessel, *Ca-Cancer J. Clin.*, 2011, **61**, 250–281.
2 E. Reddi, *J. Photochem. Photobiol., B*, 1997, **37**, 189–195.
3 J. Chen, K. Stefflova, M. J. Niedre, B. C. Wilson, B. Chance, J. D. Glickson and G. Zheng, *J. Am. Chem. Soc.*, 2004, **126**, 11450–11451.
4 Y. Choi, R. Weissleder and C.-H. Tung, *Cancer Res.*, 2006, **66**, 7225–7229.
5 G. Zheng, J. Chen, K. Stefflova, M. Jarvi, H. Li and B. C. Wilson, *Proc. Natl. Acad. Sci. U. S. A.*, 2007, **104**, 8989–8994.
6 J. Shen, Y. Zhu, X. Yang and C. Li, *Chem. Commun.*, 2012, **48**, 3686–3699.
7 L. L. Li, G. H. Wu, G. H. Yang, J. Peng, J. W. Zhao and J. J. Zhu, *Nanoscale*, 2013, **5**, 4015–4039.
8 Z. S. Qian, X. Y. Shan, L. J. Chai, J. R. Chen and H. A. Peng, *Biosens. Bioelectron.*, 2015, **68**, 225–231.
9 J. Shi, C. Chan, Y. Pang, W. Ye, F. Tian, J. Lyu, Y. Zhang and M. Yang, *Biosens. Bioelectron.*, 2015, **67**, 595–600.
10 X. Sun, Z. Liu, K. Welsher, J. T. Robinson, A. Goodwin, S. Zaric and H. Dai, *Nano Res.*, 2008, **1**, 203–212.
11 C. Wang, C. Y. Wu, X. J. Zhou, T. Han, X. Z. Xin, J. Y. Wu, J. Y. Zhang and S. W. Guo, *Sci. Rep.*, 2013, **3**, 1–8.
12 X. Wang, X. Sun, J. Lao, H. He, T. Cheng, M. Wang, S. Wang and F. Huang, *Colloids Surf., B*, 2014, **122**, 638–644.
13 C.-L. Huang, C.-C. Huang, F.-D. Mai, C.-L. Yen, S.-H. Tzing, H.-T. Hsieh, Y.-C. Lingd and J.-Y. Chang, *J. Mater. Chem. B*, 2015, **3**, 651–664.

14 M. Nurunnabi, Z. Khatun, K. M. Huh, S. Y. Park, D. Y. Lee, K. J. Cho and Y.-k. Lee, *ACS Nano*, 2013, **7**, 6858–6867.
15 Y. Chong, Y. Ma, H. Shen, X. Tu, X. Zhou, J. Xu, J. Dai, S. Fan and Z. Zhang, *Biomaterials*, 2014, **35**, 5041–5048.
16 F. Meng, W. E. Hennink and Z. Zhong, *Biomaterials*, 2009, **30**, 2180–2198.
17 Y. Q. Sun, S. Q. Wang, C. Li, P. H. Luo, L. Tao, Y. Wei and G. Q. Shi, *Phys. Chem. Chem. Phys.*, 2013, **15**, 9907–9913.
18 H. Wen, C. Dong, H. Dong, A. Shen, W. Xia, X. Cai, Y. Song, X. Li, Y. Li and D. Shi, *Small*, 2012, **8**, 760–769.
19 Y. Li, H. Dong, Y. Li and D. Shi, *Int. J. Nanomed.*, 2015, **10**, 2451–2459.
20 B. Tian, C. Wang, S. Zhang, L. Z. Feng and Z. Liu, *ACS Nano*, 2011, **5**, 7000–7009.
21 P. Huang, C. Xu, J. Lin, C. Wang, X. S. Wang, C. L. Zhang, X. J. Zhou, S. W. Guo and D. X. Cui, *Theranostics*, 2011, **1**, 240–250.
22 Y. Cho and Y. Choi, *Chem. Commun.*, 2012, **48**, 9912–9914.
23 R. Cheng, F. Feng, F. Meng, C. Deng, J. Feijen and Z. Zhong, *J. Controlled Release*, 2011, **152**, 2–12.
24 F. Li, S.-J. Park, D. Ling, W. Park, J. Y. Han, K. Na and K. Char, *J. Mater. Chem. B*, 2013, **1**, 1678–1686.
25 C. Alric, I. Miladi, D. Kryza, J. Taleb, F. Lux, R. Bazzi, C. Billotey, M. Janier, P. Perriat, S. Roux and O. Tillement, *Nanoscale*, 2013, **5**, 5930–5939.
26 K. Ma, U. Werner-Zwanziger, J. Zwanziger and U. Wiesner, *Chem. Mater.*, 2013, **25**, 677–691.